Relaxation Dynamics of Poly(methyl acrylate) at Elevated Pressure

R. Casalini,* D. Fragiadakis,[‡] and C. M. Roland

Chemistry Division, Code 6120, Naval Research Laboratory, Washington, D. C. 20375-5342, United States

ABSTRACT: Dielectric relaxation and complex heat capacity were carried out on high molecular weight poly(methyl acrylate) (PMA). The temperature was found to exert a stronger effect than density on the segmental dynamics, as reflected in the magnitudes of the scaling exponent, 2.55, and the ratio of isochoric and isobaric activation energies, 0.67. The dispersion of the heat capacity and dielectric loss were used to obtain estimates of the number of dynamically correlated segments. In accord with prior results on molecular liquids and from simulations, the extent of the dynamic correlations in PMA depends only on the relaxation time. This behavior differs from that of the fragility, which decreases with pressure, showing the disconnect between dynamic heterogeneity and fragility.
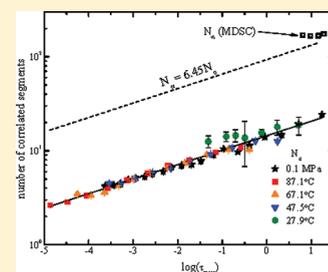
INTRODUCTION

A fascinating aspect of the dynamics of supercooled liquids and polymers is the degree to which the reorientational or segmental relaxation time, τ_{α}, governs various properties.[1,2] For example, the shape of the relaxation peak, commonly reflected in the Kohlrausch stretch exponent,[3,4] the state points associated with the dynamic crossover,[5,6] and the dynamic correlation volume[7,8] for many glass formers depend only on the relaxation time, independently of temperature and pressure. Similarly, the phase transitions of liquid crystals usually transpire at a fixed value of τ_{α}.[9] There is also a scaling relation that superposes τ_{α} measured at various temperatures and pressures, whereby any combination of temperature, T, and density, ρ, yielding a given value of T/ρ^{γ}, where γ is a material constant, will have the same relaxation time.[10−13]

Herein we examine the conformance of poly(methyl acrylate) (PMA) to these general properties. Acrylate and methacrylate polymers have been the subject of many investigations, due both to their commercial significance and to their unusual dynamics. When the pendant alkyl group in methacrylates is large, the polymers exhibit a very broad or even two glass transitions, and these materials often have unusually intense, multiple secondary relaxations.[14−20] Acrylates commonly serve as the backbone for liquid crystalline polymers.[21−24] PMA has the smallest repeat unit among acrylate polymers, which simplifies the relaxation behavior. Moreover, the effect of pressure on the fragility of PMA is among the highest reported for any polymer, which makes it an obvious choice to study the effect of pressure on relaxation properties. Despite the diminutive chain units, we find that there are two secondary relaxation processes, and the properties of the primary structural relaxation in PMA deviate from some of the general behaviors mentioned above.

EXPERIMENTAL SECTION

Poly(methyl acrylate) ($M_w \sim 4 \times 10^4$ D) was obtained from Aldrich as a toluene solution. (The molecular weight distribution is unknown; however, it has been shown that polydispersity negligibly affects T_g and the shape of the relaxation function.[25] There is a small effect on the temperature dependence of the relaxation times.[25,26]) The polymer was precipitated by addition of excess methanol, followed by vacuum drying at 323 K for more than 2 weeks. The relaxation behavior is very sensitive to small quantities of residual solvent, so that several additional weeks of drying under vacuum at 353 K were necessary to achieve invariance of the dielectric relaxation spectra, which confirmed that all solvent had been removed.

For the dielectric measurements the PMA was contained between parallel, 16 mm diameter plates, which served as electrodes. The dielectric permittivity was measured using a Novocontrol Alpha Impedance Analyzer and an Imass Time Domain Analyzer. For the measurements at atmospheric pressure, the sample was under vacuum in a closed cycle helium cryostat (Cryo Inc.), with temperature controlled to ±0.02 K. For high pressure measurements the capacitor cell was inside a pressure vessel (Harwood Engineering Inc.), with an electrically insulating oil used to transmit the pressure. The cell was isolated from the fluid by flexible Teflon and rubber seals. Pressure was applied with a manual pump in combination with an intensifier, and measured using a Sensotec transducer and Heise mechanical gauge (70 kPa accuracy). The high pressure vessel was inside a Tenney environmental chamber, with temperature controlled to within 0.1 K.

Modulated differential scanning calorimetry (MDSC) was performed using a TA Q100 calorimeter. Samples were cooled from the glass transition at a rate of $q = 0.5$ K/min, with temperature modulation 1 K and modulation periods of $T_t = 40, 60, 90$, and 120 s. The heat capacity was calibrated for each modulation period using a sapphire sample. The error in the MDSC measurements due to the temperature dependence of the heat capacity at the glass transition (nonstationary thermal response) can be estimated from the relative change of the heat capacity, $\Delta c_P^*/c_P^*$, over one modulation period. This is given by $\Delta c_P^*/c_P^* \approx (dc_P^*/d\langle T \rangle)qT_t/c_P^*$,[27] and for the measurements reported herein we estimate $\Delta c_P^*/c_P^* \leq 0.02$.

RESULTS AND DISCUSSION

Dielectric Measurements. Representative dielectric spectra of PMA at atmospheric pressure are shown in Figure 1. Three relaxation processes are evident, the α transition (local segmental
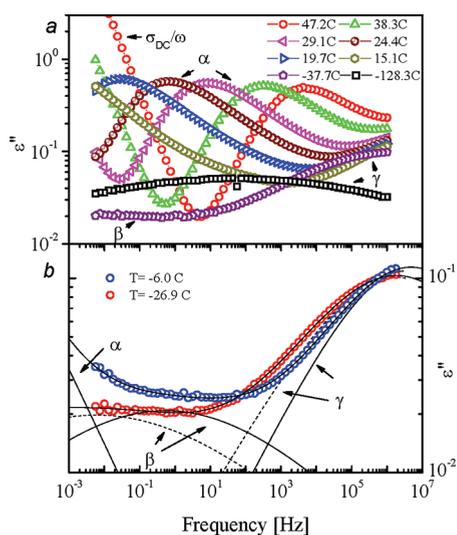
Figure 1. (a) Dielectric loss of PMA at atmospheric pressure and various temperatures. The β process is obscured by other, more intense relaxation peaks. (b) Dielectric loss of PMA at atmospheric pressure and two temperatures below T_g. The weak β process is indicated. The contribution of the three relaxations are shown by the fitted curves (dotted lines for -26.9 °C and solid lines for -6.0 °C).

dynamics) observed above T_g and two secondary relaxations, the higher frequency of which is more intense and referred to as the γ process. Above T_g this γ peak shifts to frequencies beyond the measurement range. The lower frequency of the two secondary relaxations, the β relaxation, is very weak. Below T_g it is partially submerged toward higher frequency by the tail of the α process and becomes completely masked above T_g. To show more clearly the β process, two spectra measured below T_g are shown in figure 1b. The real and imaginary part of the spectra were fit to the superposition of three relaxation functions (although the contribution from the α process becomes negligible below T_g), a Kohlrausch—Williams—Watts (KWW) and two Cole—Cole (CC)[28] functions

$$\varepsilon^*(\omega) = \varepsilon_\infty + \Delta\varepsilon_\alpha L_{i\omega}\left[-\frac{\mathrm{d}\varphi_\alpha(t,\tau_\alpha)}{\mathrm{d}t}\right]$$

$$+ \frac{\Delta\varepsilon_\beta}{(1 + i\omega\tau_\beta)^{\alpha_{CC}^\beta}}$$

$$+ \frac{\Delta\varepsilon_\gamma}{(1 + i\omega\tau_\gamma)^{\alpha_{CC}^\gamma}}$$

with $\varphi_\alpha(t,\tau_\alpha) = \exp[-(t/\tau_\alpha)^{\beta_{KWW}}]$ (1)

where $L_{i\omega}$ indicates the Laplace transform, ε_∞ is the high frequency permittivity, τ_i are the relaxation times, $\Delta\varepsilon_i$ are the dielectric strengths, and α_{CC} and β_{KWW} are shape parameters. The Laplace transform of the KWW function was done numerically using the method of Macdonald.[29] Equation 1 assumes the processes are independent. Previous investigations of the dynamics of PMA[30,31] did not report the β process, probably because of its small amplitude.

Although the β process is close to but faster than the α relaxation, reminiscent of a Johari—Goldstein (J—G) process,[32] determination of its relaxation time has a large uncertainty due to the relatively weak dielectric strength. Also for this reason we could not assess its properties in terms of those expected for a J—G relaxation. The latter has been observed, for example, in
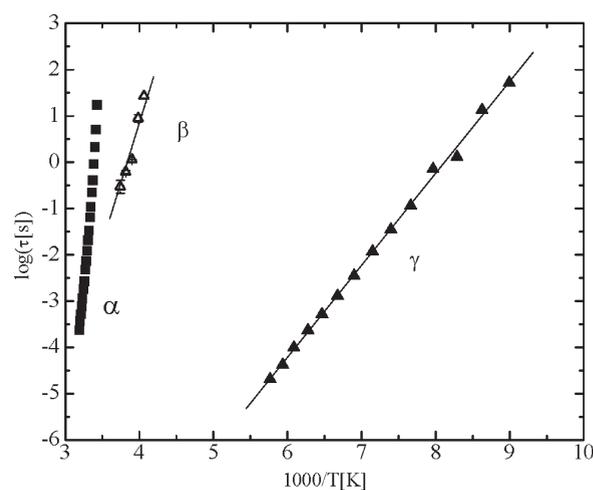
Figure 2. Arrhenius plot of the relaxation times of the three dielectric relaxations in PMA.

poly(methyl methacrylate) (PMMA);[33] a discussion of the β process in other acrylates and methacrylates is presented at the end of this section. The relaxation times of both secondary relaxations exhibit Arrhenius behavior (Figure 2), with activation energies below T_g equal to 80 ± 20 and 38.0 ± 0.4 kJ mol^{-1} for the β and γ processes, respectively. Certainly for the γ process this activation energy is too small to be a J—G relaxation,[34] indicating that the underlying motion probably involves noncooperative rearrangements of only some atoms in the repeat unit of PMA.

The α process shows the usual non-Arrhenius behavior, with an effective activation energy increasing with decreasing temperature. At the longest measured τ_α (17.2 s), the effective activation energy is 660 kJmol^{-1}, which corresponds to a steepness index, $m = \partial\log(\tau)/\partial(T_a/T)|_{T=T_s}$, equal to $118+/-3$. (This choice of τ_α avoids extrapolation, reducing the error in the determination of m.) Thus, PMA is one of the more fragile amorphous polymers. Only poly(vinylethylene) ($m = 140$) and poly(vinyl chloride) ($m = 160$) have steeper T_g-normalized Arrhenius slopes.[35,36] (Cross-linking increases the steepness index and can yield even higher values of m.[37,38]) The peak breadth is generally anticorrelated with m,[39] and for PMA we find β_{KWW} in the range 0.37—0.41 (Figure 3). According to the general pattern for polymers,[39] this β_{KWW} gives a rough estimate of $m \sim 115$, which is consistent with the present result. From mechanical measurements on PMA, $m = 106$ and $\beta_{KWW} = 0.41$ at $T_g = 287$ K.[40] These values are close to our dielectric results, although differences are inherent to the two spectroscopies.[41,42]

Heat Capacity Measurements. The real and imaginary parts of the heat capacity (modulation period = 60 s) are shown in Figure 4.[43,44] The breadth (fwhm) of the C_P'' transition interval, $2\delta T$, was determined by fitting a Gaussian function to the peak. The values of T_g and δT for the four modulation periods are listed in Table 1. Defining the relaxation time as $\tau^* = (2\pi f)^{-1}$, where $f(T)$ is the modulation frequency at the temperature of the maximum in $C_P''(T)$, we calculated the $\tau^*(T)$ shown in Figure 5. Also included are the dielectric relaxation times defined in the same manner from isochronal dielectric peaks, $\varepsilon''(T)$. Note that τ^* from the dielectric data are larger than the values from calorimetry. τ_α determined from fitting eq 1 to the dielectric spectra, $\varepsilon''(\omega)$, are also larger than the calorimetric τ^* (cf. Figures 2 and 5).

We did not determine δT from the isochronal dielectric measurements because the background loss introduces large error.

For example, a change in the background of 0.1, which is only 6% of the peak maximum, changes the computed breadth by more than 25%. This background is due to the intense γ process, as seen in the isochronal spectra at the lowest temperatures in Figure 6. However, this background intensity introduces negligible error (<0.5%) in the value of the peak maximum.

Dynamic Heterogeneity. The intermolecularly cooperative dynamics involves correlations both in time and in space; thus, this dynamic heterogeneity cannot be quantified directly from linear relaxation measurements. However,
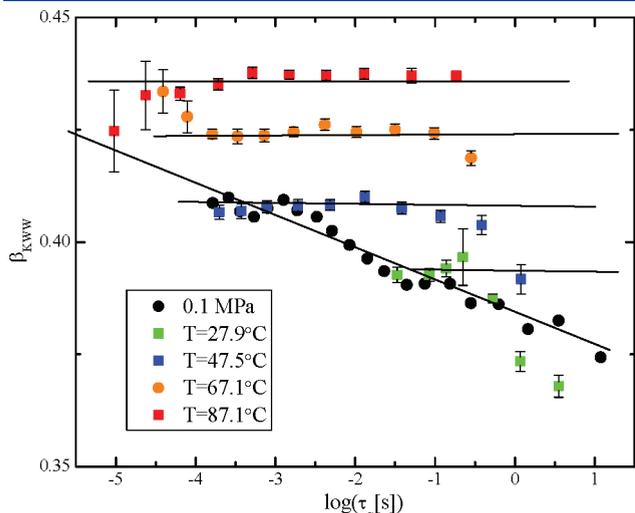
Figure 3. Kohlrausch exponent for the α process in PMA versus $\log(\tau_\alpha)$ at atmospheric pressure for four isotherms (291.6 K < T < 313.9 K). The lines are to guide the eye.
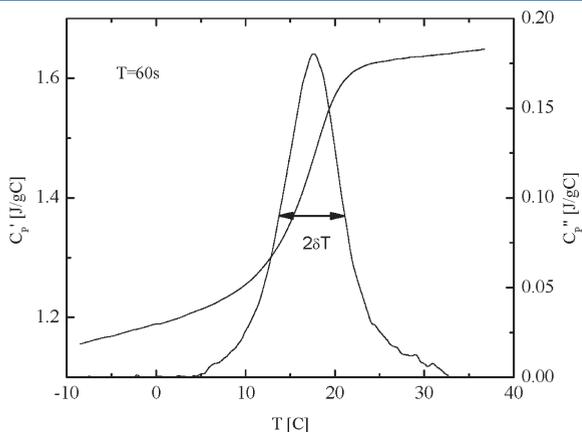
Figure 4. Real and imaginary parts of the heat capacity of PMA for a 60 s modulation period. Before calculating C_P'', the phase angle was corrected as discussed by Weyer et al.[43,44]

Berthier et al.[45] derived an approximate formula for the number of dynamically correlated molecules, or segments in the case of polymers, by assuming the dynamics are driven mainly by temperature, rather than density, fluctuations. (This assumption is more correct for polymers than molecular liquids.[1,13]) For relaxations having the Kohlrausch form, the number of correlated segments is[46]

$$N_c = \frac{R}{\Delta c_P m_0} \left(\frac{\beta_{KWW}}{e}\right)^2 \left(\frac{d \ln \tau_\alpha}{d \ln T}\right)^2 \qquad (2)$$

in which Δc_P is the isobaric heat capacity increment at T_g, m_0 is the monomer molecular weight (86 g/mol for PMA), R is the gas constant, and e is Euler's number. At least near the glass transition, molecular dynamic simulations have shown that the approximate N_c from eq 2 is quite close to the rigorous value determined from the four-point dynamic susceptibility.[45,47] The number of dynamically correlated segments calculated from the dielectric measurements is plotted in Figure 7. It is seen that N_c depends only on the relaxation time, independent of T and P. This finding agrees with our earlier results for four molecular glass formers[8] and for simulated Lennard-Jones particles.[7] In the investigated range we find that N_c for PMA varies linearly with $\log \tau_\alpha$. Note that because the dependence of the heat capacity on pressure is negligible, we used the atmospheric pressure value of Δc_P^{-1} for all five data sets in Figure 7; that is, we assumed Δc_P^{-1} is constant with pressure.

An alternative formula derived by Donth[48] is similar to eq 2

$$N_\alpha(T) = \frac{RT^2 \Delta c_P^{-1}}{m_0(\delta T^2)} \qquad (3)$$

Using the heat capacity data in Table 1, N_α at atmospheric pressure is calculated and shown in Figure 7. Note that in both eqs 2 and 3, the choice of $\Delta c_P^{-1} [(1/c_P)_{liq} - (1/c_P)_{glass} \approx \Delta c_P/c_P^2]$, rather than $(\Delta c_P)^{-1}$, is arbitrary, affecting the absolute magnitude of N_c or N_α, but not their variation with T, P, or τ_α.[49] From Table 1 $\Delta c_P^{-1}/\Delta c_P \approx 0.5$. The relation[50]

$$\delta T \approx \frac{\delta \ln \tau_\alpha}{\partial \ln \tau_\alpha/\partial T} = \frac{1.07T}{\beta_{KWW}} \left(\frac{d \ln \tau_\alpha}{d \ln T}\right)^{-1} \qquad (4)$$

together with eq 2 gives

$$N_\alpha = 6.45 N_c \qquad (5)$$

This equation is in reasonable accord with the N_α in Figure 7. Thus, the two methods of determining the number of dynamically correlated segments agree both in magnitude and in their dependence on τ_α.

By assuming that temperature and polarization fluctuations have the same spectral shape, Saiter and co-workers[51] applied eq 3 to dielectric measurements, with δT taken as the temperature spread of the α peak measured at constant frequency. However, the interference from the γ process, discussed above, precluded accurate determination of δT in this manner.

Table 1

modulation period [s]	T_g [K]	$V(T_g)$ [cm³/g]	$\rho(T_g)$ [g/cm³]	$2\delta T$ [C]	$C_{P,liq}$ [J/(g C)]	$C_{P,glass}$ [J/(g C)]	ΔC_P [J/(g C)]	$\Delta(1/C_P)$ [(g C)/J]
40	291.54	0.8179	1.223	5.81	1.55	1.22	0.33	0.174
60	290.63	0.8174	1.223	5.94	1.61	1.25	0.36	0.179
90	289.77	0.8170	1.224	5.93	1.65	1.27	0.38	0.181
120	289.44	0.8168	1.224	5.86	1.66	1.27	0.39	0.185
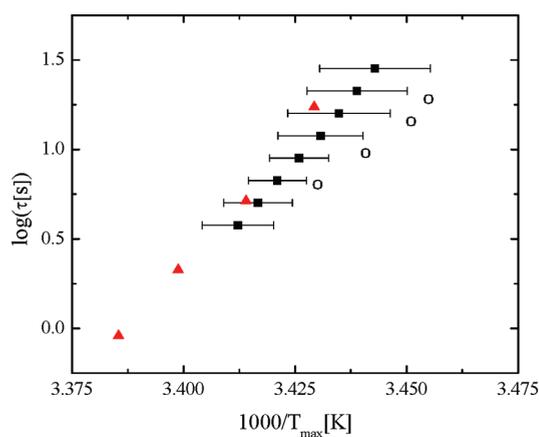
Figure 5. Relaxation times τ $(1/2\pi f_{max})$ for PMA versus the inverse of the temperature of the peak maximum determined from the fit of a Gaussian to the peak in the isochronal dielectric loss (squares) and the peak in the MDSC $C_P''(T)$ (circles). The relaxation times (circles) determined from the fit of eq 1 to the dielectric spectra measured in the frequency domain are also shown (see Figure 2).
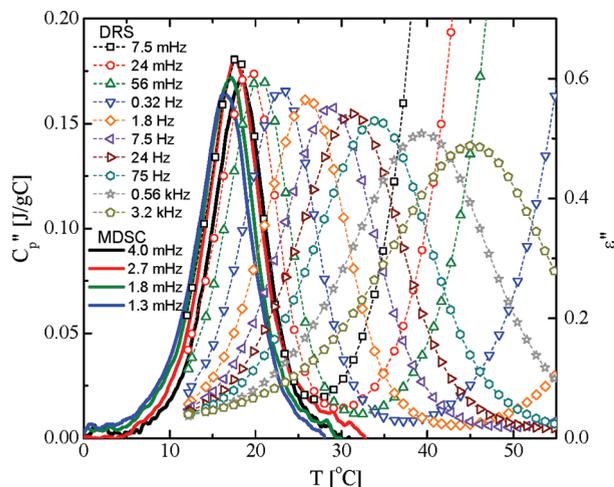
Figure 6. Isochronal response of PMA measured by MDSC (solid lines) and dielectrically (symbols with dotted lines) at the indicated frequencies. For a given frequency, the calorimetry peak is at higher temperature. Note the rise in $\varepsilon''(T)$ at lower T due to the increasing contribution of the γ process.

Thermodynamic Scaling. PVT data from the literature[52] were used to determine the equation of state (EoS) for the PMA

$$V(T,P) = 0.808(\exp[6.64 \times 10^{-4}T])$$
$$\times \left[1 - 0.0894 \ln\left(1 + \frac{P}{247.84 \exp[-4.26 \times 10^{-3}T]}\right)\right] \quad (6)$$

where T is in °C. Plotting τ_α versus volume (Figure 8) shows that the segmental dynamics do not depend uniquely on V (or T). However, for all nonassociated organic liquids and polymers, it has been found that[10–12]

$$\tau_\alpha = \mathscr{T}(TV^\gamma) \quad (7)$$

where γ is a material constant and $\mathscr{T}$ is a function. As shown in Figure 9, the segmental relaxation times of PMA conform well to
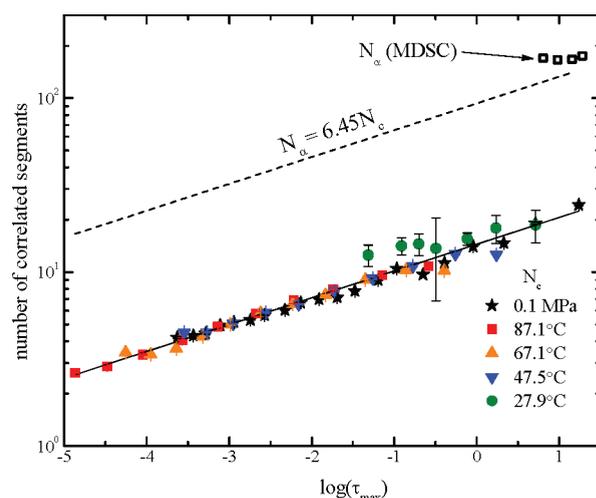
Figure 7. N_c and N_α for PMA at atmospheric pressure and N_c at high pressure. The solid line is a linear fit to the N_c data; the dotted line is this fit after adjusting by the factor from eq 5.
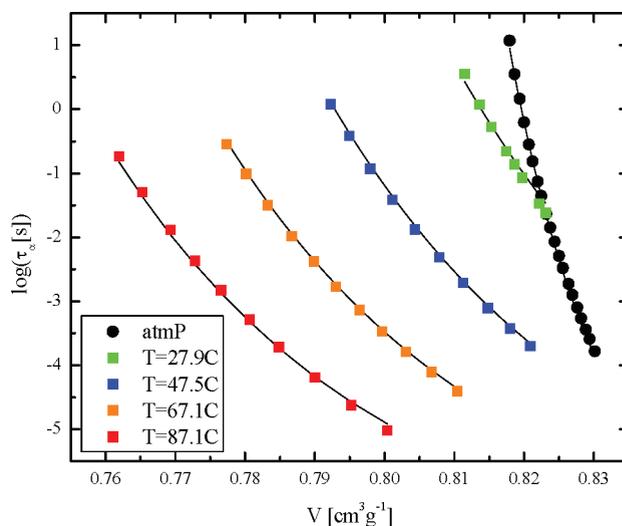
Figure 8. Dependence of the segmental relaxation time of PMA on the specific volume at atmospheric pressure and for four isotherms (291.6 K < T < 313.9 K). The solid lines represent the fit of the scaling function derived from the Avramov model (eq 9).

eq 7 with γ = 2.55. In the inset of the same figure is the scaled relaxation time, τ_{PCS}, of PMA measured using photon correlation spectroscopy (PCS) by Fytas et al.,[53] using the same EOS as for the dielectric data. The PCS data scale quite well for γ = 2.75, which is close to the value of γ of the dielectric measurements. This confirms previous observations that the values of γ determined for different observables (dielectric relaxation, viscosity, etc.) agree reasonably well.

Using the scaling function (eq 7), N_c can calculated as[8]

$$N_c(T,V) = \frac{R}{\Delta c_P}\frac{N_A}{m_o}\left(\frac{\beta_{KWW}}{e}\right)^2\left(\frac{d \ln \tau_\alpha}{dTV^\gamma}TV^\gamma(1 + \gamma\alpha_P T)\right)^2 \quad (8)$$

From eq 8 it follows that for N_c to be a function of TV^γ (or equivalently of τ_α), β_{KWW} should depend only on TV^γ, independently of T and P, and the product $\alpha_P T$ should be constant.
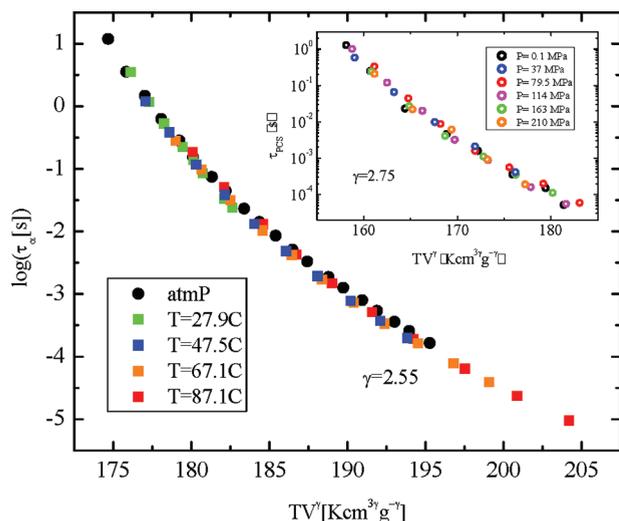
Figure 9. Scaling plot of the segmental relaxation time of PMA, with $\gamma = 2.55$. The inset is the scaling plot for the relaxation time measured using photon correlation spectroscopy, τ_{PCS}, by Fytas et al.[53] with the value of γ indicated.
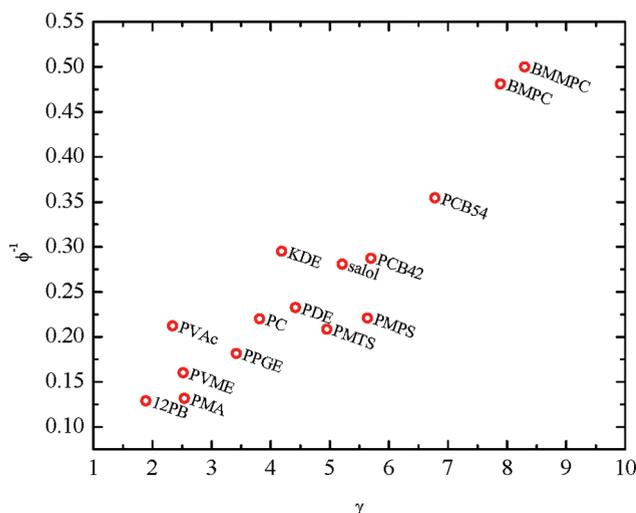
Figure 10. Correlation of the parameters ϕ and γ for different materials.

For the PMA herein, neither condition is satisfied: β_{KWW} is not a function of τ_α (Figure 3), and $\alpha_P T_g$ decreases from 0.19 at atmospheric pressure to ~0.15 at the highest pressure (550 MPa). However, because N_c is a function of τ_α, these variations of β_{KWW} and $\alpha_P T_g$ evidently compensate each other.

Starting with the Avramov entropy model of the dynamics,[54] we previously derived a form for the (otherwise unspecified) function $\mathscr{T}$ in eq 7[55]

$$\log(\tau_\alpha) = \log \tau_o + \left(\log(e) \frac{A}{TV^\gamma} \right)^\phi \tag{9}$$

where τ_o, A, and ϕ are constants. This function requires only one more parameter than, for example, the Vogel–Fulcher[1] or Avramov equation[54] used to describe the temperature dependence of τ_α at constant pressure. Moreover, the parameters in eq 9 are T- and V-independent; that is, fitting does not have to be
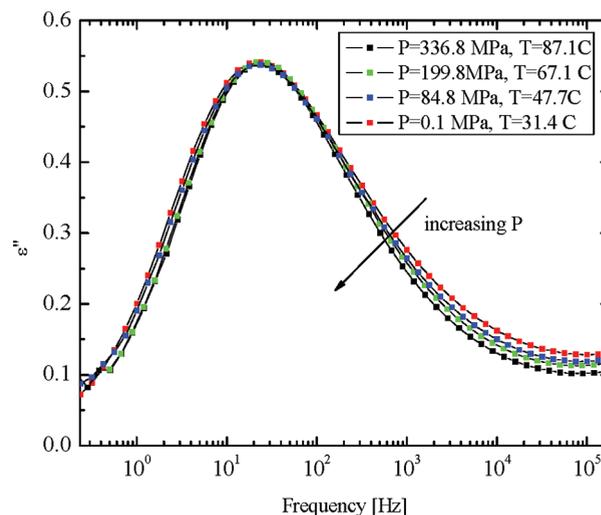
Figure 11. Dielectric loss peak in PMA at state points for which τ_α is constant. The ordinate values were normalized to superpose the peak. The spectra narrow with increasing pressure, with β_{KWW} in the range $0.40 < \beta_{KWW} < 0.44$.

carried out individually for each isotherm. The fits of eq 9 to the PMA τ_α data are shown in Figure 8; $\log(\tau_o) = -7.5 \pm 0.2$, $A = 534 \pm 8$ K cm$^{3\gamma}$ g$^{-\gamma}$, $\gamma = 2.54 \pm 0.01$, and $\phi = 7.6 \pm 0.3$. Previously we pointed out that γ and ϕ are not independent but show an inverse proportionality.[56] In Figure 10 these values of ϕ and γ are plotted, along with those for other materials; the anticorrelation of ϕ and γ is evident. Thus, the parameter ϕ is to some extent redundant, and eq 9 could be rewritten substituting for ϕ with a function of γ.[57] Although this relationship between ϕ and γ is strictly empirical, it does indicate that the single parameter γ governs the temperature and pressure behavior (e.g., fragility and activation volume) of the segmental dynamics.

A measure of the relative degree to which volume and temperature control the dynamics is the ratio of the isochoric (E_V) and isobaric (E_P) activation energies. For PMA Williams[31] reported $E_V/E_P \geq 0.78$, which is larger than one-half, implying temperature is the more dominant control parameter. The value of this ratio can be calculated from the scaling exponent using[10,58]

$$\frac{E_V}{E_P} = (1 + \gamma\alpha_P T)^{-1} \tag{10}$$

Unlike γ, E_V/E_P varies with temperature. From this equation we calculate at $T_g = 289$ K ($\tau_\alpha = 10^2$ s) $E_V/E_P = 0.67$. This is smaller than the earlier result[31] possibly because the molecular weight used in the prior study (2×10^6 D) was much larger than herein; chain ends accentuate the effect of volume on τ_α[11] rendering E_V/E_P smaller.

A general property of nonassociating liquids and polymers is isochronal superpositioning,[3,4,59] which refers to the invariance of the shape of the relaxation peak to changes in T or P, as long as τ_α is constant. However, for the α process in PMA β_{KWW} is almost independent of pressure at constant T, which means that at fixed τ_α, the dielectric loss peak becomes narrower with increasing pressure (corresponding to increasing temperature (Figure 3)). This breakdown of isochronal superpositioning in PMA is illustrated in Figure 11. Such behavior has been observed before only for hydrogen bonded liquids, a result of the concentration of H-bonds changing with T and P, although in those cases spectra broaden with increasing pressure.[3,4,60] However,
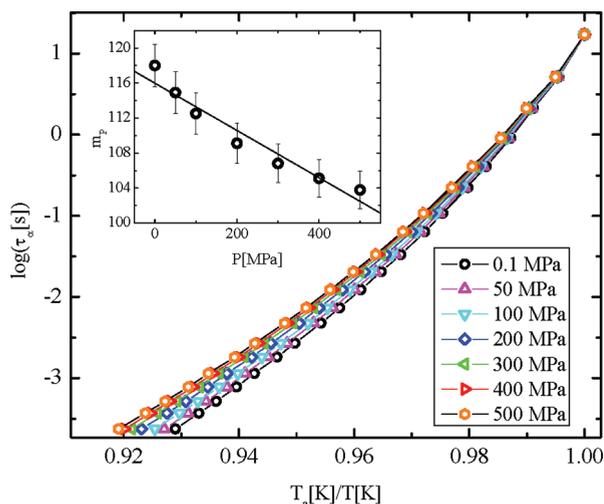
Figure 12. Segmental relaxation times of PMA versus T_a-normalized temperature for the indicated pressures. The steepness of the curves decreases with pressure (inset), with $dm/dP = -27 \pm 5$ GPa^{-1} at ambient pressure as determined from the linear fit (solid line).
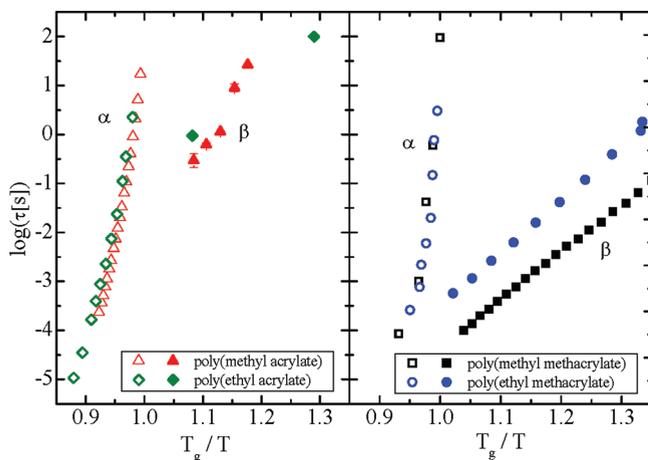
Figure 13. $\alpha-$ (open symbols) and $\beta-$ (solid symbols) relaxation times for PMA, PMMA, PEA and PEMA versus the inverse temperature normalized to the glass temperature. The β process for the acrylate polymers is several orders of magnitude closer to the α process than in the poly(methyl acrylate)s. Data for PMMA from ref 61 and for PEA and PEMA from ref 62.

there is no hydrogen bonding in PMA. Possibly the unusual behavior reflects the contribution of a secondary process. Although the intensity of the β peak is more than 10-fold smaller than that of the α at low temperatures where the peaks are resolved, at higher T in their overlap region the dielectric strength of the β process is expected to increase significantly. Measurements on lower molecular weight PMA could clarify this issue, because that would give greater separation between the structural and secondary relaxation peaks. Another possibility is that the α process is actually the superposition of two processes having very similar temperature behavior and almost identical pressure behavior. That would imply an unresolved J—G relaxation, although this hypothesis is speculative, based only on the breakdown of isochronal superpositioning.

Finally, using the scaling property and the EoS, we calculate for various pressures the change in the relaxation time with temperature by numerically solving the equation $T_1(V(T_1,P_{atm}))^\gamma = TV(T,P)^\gamma$,

where T_1 is the temperature at which τ_α was measured at atmospheric pressure.[35] Isobars calculated in this manner for six different pressures between 50 and 500 MPa are displayed in Figure 12 in the form of fragility plots. From the linear fit of m vs P we find $dm/dP = -27 \pm 5$ GPa^{-1}. This is significantly smaller than the pressure coefficient reported previously from more limited data, -180 MPa^{-1}.[36] Nevertheless, the change of fragility with pressure for PMA is among the largest of all liquids and polymers.[13]

Because m changes with pressure, but N_c is independent of P at fixed τ_α (Figure 7), there can be no direct relationship between N_c and fragility. We had previously demonstrated this lack of correlation between these two quantities at atmospheric data for various materials;[8] at least for PMA, varying pressure shows that m and N_c are uncorrelated even within a single material.

Comparison with Other Acrylates and Methacrylates. Although the molecular structures of PMMA and PMA differ only by a pendant methyl group, this affects the chain rigidity and local packing enough to change T_g by more than 100 K. However, the β relaxation times for PMMA[61] although larger, are relatively close to those of PMA (between one and two decades). Recently, a similar scenario was reported for poly(ethyl acrylate) (PEA) and poly(ethyl methacrylate) (PEMA).[62] The τ_β for the acrylate polymer is about 1.5 decades faster than for the methacrylate counterpart and has a comparable activation energy. Also, for both PEA and PMA, the dielectric strength of the β process is much smaller than that of the α process, with a third, intense process (γ process) at much higher frequency. When the relaxation times are normalized to the glass transition (Figure 13), the α and β processes are more than 3 decades closer for the acrylates than for the methacrylates.

Schmidt-Rohr et al.[33] used NMR and MD simulations to determine that the β process in PMMA corresponds to flipping of the bulky pendant group. Because of the asymmetry of this side group, its reorientation requires rearrangement of the entire repeat unit. It can be speculated that this flipping of the bulky side group is responsible for the γ process in polyacrylates. In PMMA and PEMA the molecular structure constrains this motion, causing it to become cooperative. The weaker intensity and longer τ_β (Figure 13) for the β process in the acrylates indicates noncooperative motion of the main chain, consistent with the smaller separation between τ_α and τ_β.

■ SUMMARY

From PVT and dielectric relaxation data at ambient and elevated pressures, and from modulated calorimetry experiments on a high molecular weight PMA, the following results were obtained:

1. A new secondary relaxation was discovered, which is much weaker in dielectric strength than the higher frequency secondary process, and has an activation energy almost 2-fold higher. This process may be the J—G relaxation in PMA, as a comparison with the PMMA relaxation map suggests.
2. The number of dynamically correlated segments was estimated from both dielectric and DSC data, the two methods yielding consistent results. In agreement with previous work on small molecule liquids, the dynamic correlation volume is constant for all state points having a given value of the α relaxation time.
3. Segmental relaxation times for the PMA conform to density scaling. From the scaling exponent $\gamma = 2.55$, the activation energy ratio is calculated. Its magnitude, $E_V/E_P = 0.67$ at T_g, indicates a more dominant role of temperature over volume on the structural dynamics.

4. The α relaxation dispersion in PMA deviates from the isochronal superpositioning found for virtually all other nonassociated liquids and polymers. The deviation may be due to overlapping of a secondary process.

5. The fragility of PMA changes strongly with pressure, $dm/dP = -27 \pm 5$ GPa^{-1}, the negative sign of the pressure coefficient in accord with other materials lacking H-bonds. In consideration of item 2 above, this nonzero pressure dependence affirms the lack of correlation between fragility and dynamic heterogeneity.

Notes

‡National Research Council/Naval Research Laboratory Postdoctoral Fellow.

■ ACKNOWLEDGMENT

■ REFERENCES

(1) Roland, C. M. *Macromolecules* **2010**, *43*, 7875.
(2) Roland, C. M. *Soft Matter* **2008**, *4*, 2316.
(3) Ngai, K. L.; Casalini, R.; Capaccioli, S.; Paluch, M.; Roland, C. M. *J. Phys. Chem. B* **2005**, *109*, 17356.
(4) Ngai, K. L.; Casalini, R.; Capaccioli, S.; Paluch, M.; Roland, C. M. *Adv. Chem. Phys.* **2006**, *133*, 497.
(5) Casalini, R.; Paluch, M.; Roland, C. M. *J. Chem. Phys.* **2003**, *118*, 5701.
(6) Casalini, R.; Roland, C. M. *Phys. Rev. B* **2005**, *71*, 014210.
(7) Coslovich, D.; Roland, C. M. *J. Chem. Phys.* **2009**, *131*, 151103.
(8) Fragiadakis, D.; Casalini, R.; Roland, C. M. *J. Phys. Chem. B* **2009**, *113*, 13134.
(9) Urban, S.; Roland, C. M. *J. Non-Cryst. Sol.* **2011**, *357*, 740.
(10) Casalini, R.; Roland, C. M. *Phys. Rev. E* **2004**, *69*, 062501.
(11) Alba-Simionesco, C.; Cailliaux, A.; Alegria, A.; Tarjus, G. *Europhys. Lett.* **2004**, *68*, 58.
(12) Dreyfus, C.; Le Grand, A.; Gapinski, J.; Steffen, W.; Patkowski, A. *Eur. J. Phys.* **2004**, *42*, 309.
(13) Roland, C. M.; Hensel-Bielowka, S.; Paluch, M.; Casalini, R. *Rep. Prog. Phys.* **2005**, *68*, 1405.
(14) McCrum, N. G.; Read, B. E.; Williams, G. *Anelastic and Dielectric Effects in Polymeric Solids*; Dover, Inc.: New York, 1991.
(15) Beiner, M.; Schröter, K.; Hempel, E.; Reissig, S.; Donth, E. *Macromolecules* **1999**, *32*, 6278.
(16) Floudas, G.; Placke, P.; Stepanek, P.; Brown, W.; Fytas, G.; Ngai, K. L. *Macromolecules* **1995**, *28*, 6799.
(17) Hempel, E.; Beiner, M.; Huth, H.; Donth, E. *Thermochim. Acta* **2002**, *391*, 219.
(18) Floudas, G.; Štepánek, P. *Macromolecules* **1998**, *31*, 6951.
(19) Mpoukouvalas, K.; Floudas, G.; Williams, G. *Macromolecules* **2009**, *42*, 4690.
(20) Arbe, A.; Genix, A. C.; Arrese-Igor, S.; Colmenero, J.; Richter, D. *Macromolecules* **2010**, *43*, 3107.
(21) Yang, C. A.; Wang, Q.; Xie, H. L.; Zhong, G. Q.; Zhang, H. L. *Liq Cryst.* **2010**, *37*, 1339.
(22) Cui, L.; Tong, X.; Yan, X. H.; Liu, G. J.; Zhao, Y. *Macromolecules* **2004**, *37*, 7097.
(23) Ortiz, C.; Ober, C. K.; Kramer, E. J. *Polymer* **1998**, *39*, 3713.
(24) Whale, E. A.; Davis, F. J.; Mitchell, G. R. *J. Mater. Chem.* **1996**, *6*, 1479.
(25) Bogoslovov, R. B.; Hogan, T. E.; Roland, C. M. *Macromolecules* **2010**, *43*, 2904.
(26) Dalle-Ferrier, C.; Simon, S.; Zheng, W.; Badrinarayanan, P.; Fennell, T.; Frick, B.; Zanotti, J. M.; Alba-Simionesco, C. *Phys. Rev. Lett.* **2009**, *103*, 185702.
(27) Merzlyakov, M.; Schick, C *Macromolecules* **2000**, *61*, 649.
(28) *Broadband Dielectric Spectroscopy*; Kremer, F., Schonhals, A., Eds.; Springer-Verlag: Berlin, Heidlberg, and New York, 2003.

(29) Ross Macdonald, J. J. *Non-Cryst. Sol.* **1997**, *95*, 212.
(30) Ishida, Y. *Kolloid Z.* **1961**, *124*, 174.
(31) Williams, G. *Trans. Faraday Soc.* **1964**, *60*, 1556.
(32) Ngai, K. L.; Paluch, M. *J. Chem. Phys.* **2004**, *120*, 857.
(33) Schmidt-Rohr, K.; Kulik, A. S.; Beckham, H. W.; Ohlemacher, A.; Pawelzik, U.; Boeffel, C.; Spiess, H. W. *Macromolecules* **1994**, *27*, 4733.
(34) Ngai, K. L.; Capaccioli, S. *Phys. Rev. E* **2004**, *69*, 031501.
(35) Casalini, R.; Roland, C. M. *Phys. Rev. E* **2005**, *72*, 031503.
(36) Huang, D.; Colucci, D. M.; McKenna, G. B. *J. Chem. Phys.* **2002**, *116*, 3925.
(37) Roland, C. M. *Macromolecules* **1994**, *27*, 4242.
(38) Roland, C. M.; Roland, D. F.; Wang, J.; Casalini, R. *J. Chem. Phys.* **2005**, *123*, 204505.
(39) Bohmer, R.; Ngai, K. L.; Angell, C. A.; Plazek, D. J. *J. Chem. Phys.* **1993**, *99*, 4201.
(40) Plazek, D. J.; Ngai, K. L. *Macromolecules* **1991**, *24*, 1222.
(41) Buchenau, U.; Ohl, M.; Wischnewski, A. *J. Chem. Phys.* **2006**, *124*, 094505.
(42) Matsumiya, Y. 6th International Conf. on Broadband Dielectric Spectroscopy and its Applications, Madrid, Sept 2010.
(43) Weyer, S.; Hensel, A.; Schick, C. *Thermochim. Acta* **1997**, *304/305*, 267–275.
(44) *Applications to Polymers and Plastics*; Cheng, S. Z. D., Ed.; Handbook of thermal analysis and calorimetry, Vol. 3; Elsevier Science: Amsterdam, 2002.
(45) Berthier, L.; Biroli, G.; Bouchaud, J.-P.; Cipelletti, L.; El Masri, D.; L'Hote, D.; Ladieu, F.; Pierno, M. *Science* **2005**, *310*, 1797. Berthier, L.; Biroli, G.; Bouchaud, J.-P.; Kob, W.; Miyazaki, K.; Reichman, D. R. *J. Chem. Phys.* **2007**, *126*, 184503.
(46) Capaccioli, S.; Ruocco, G.; Zamponi, F. *J. Phys. Chem. B* **2008**, *112*, 10652.
(47) Roland, C. M.; Fragiadakis, D.; Coslovich, D.; Capaccioli, S.; Ngai, K. L. *J. Chem. Phys.* **2010**, *133*, 124507.
(48) Donth, E. *J. Non-Cryst. Solids* **1982**, *53*, 325.
(49) Dalle-Ferrier, C.; Thibierge, C.; Alba-Simionesco, C.; Berthier, L.; Biroli, G.; Bouchaud, J.-P.; Ladieu, F.; L'Hôte, D.; Tarjus, G. *Phys. Rev. E* **2007**, *76*, 041510.
(50) Fragiadakis, D.; Casalini, R.; Bogoslovov, R. B.; Robertson, C. G.; Roland, C. M. *Macromolecules* **2011**, *44*, 1149.
(51) Saiter, A.; Delbreilh, L.; Couderc, H.; Arabeche, K.; Schönhals, A.; Saiter, J.-M. *Phys. Rev. E* **2010**, *81*, 014805.
(52) Zoller, P.; Walsh, D. J. *Standard Pressure-Vol.-Temperature Data for Polymers*; Technomic: Lancaster, PA, 1995.
(53) Fytas, G.; Patkowski, A.; Meier, G.; Dorfmüller, Th. *J. Chem. Phys.* **1984**, *80*, 2214.
(54) Avramov, I. *J. Non-Cryst. Solids* **2005**, *351*, 3163.
(55) Casalini, R.; Mohanty, U.; Roland, C. M. *J. Chem. Phys.* **2006**, *125*, 014505.
(56) Casalini, R.; Roland, C. M. *J. Non-Cryst. Solids* **2007**, *353*, 3936.
(57) Casalini, R.; Capaccioli, S.; Roland, C. M. *J. Phys. Chem. B* **2006**, *110*, 11491.
(58) Casalini, R.; Roland, C. M. *Colloid Polym. Sci.* **2004**, *283*, 107.
(59) Roland, C. M.; Casalini, R.; Paluch, M. *Chem. Phys. Lett.* **2003**, *367*, 259.
(60) Paluch, M.; Casalini, R.; Hensel-Bielowka, S.; Roland, C. M. *J. Chem. Phys.* **2002**, *116*, 9839.
(61) Bergman, R.; Alvarez, F.; Alegría, A.; Colmenero, J. *J. Chem. Phys.* **1998**, *109*, 7546.
(62) Spanoudaki, A.; Panagopoulou, A.; Gouvierou, N.; Pradas, M. M.; Gomez-Ribelles, J. L.; Pissis, P. 4th Workshop on Non-Equilibrium Phenomena in Supercooled Fuids, Glasses and Amorphous Materials, September 17—22, 2006, Pisa, IT.